Influence of low-contrast sub-wavelength grating shape on polarization characteristics of GaN-based light-emitting diode emissions

Yuusuke Takashima,[a] Ryo Shimizu,[a] Masanobu Haraguchi,[a,b] Yoshiki Naoi[a,b]

[a]Tokushima University, Graduate School of Advanced Technology and Science, 2-1 Minami-josanjima, Tokushima 770-8506, Japan
[b]Tokushima University, Institute of Technology and Science, 2-1 Minami-josanjima, Tokushima 770-8506, Japan

Abstract. We analytically investigated the influence of grating shape on polarization characteristics of the emission from a GaN-based light-emitting diode with a low-contrast sub-wavelength grating (SWG), such as SiO_2-SWG. The electromagnetic field distribution, calculated using the finite difference time domain method, predicted that the polarization characteristics strongly depend on the grating-side slope. A trapezoid SiO_2-SWG was fabricated on the GaN-based-LED using electron beam lithography. The optical characteristics of the electroluminescence agreed with those theoretically predicted, and we succeeded in demonstrating the influence of grating shape on the polarization of LED emission.

Keywords: sub-wavelength grating, mode eigenstates, LED, polarization, grating shape.

Address all correspondence to: Yuusuke Takashima, Tokushima University, Graduate School of Advanced Technology and Science, 770-8506, Tokushima, Japan, Tel: +81-88-656-7447; Fax: +81-88-656-7447; E-mail: takashima@ee.tokushma-u.ac.jp

1   Introduction

GaN-based light-emitting diodes (LEDs) have been developed as solid-state light sources suitable for saving energy, environmental safeguards, and device integration compared to traditional light sources.[1] Although both the output power and light conversion efficiency in LEDs have improved significantly, further improvements of their characteristics may bring about the development of novel integrated applications. Highly polarized LEDs are extremely well-suited for integrated devices including imaging tools, sensors, and liquid crystal backlighting systems, which require a compact polarization-controlling device with high transmittance. Many attempts to develop polarized LEDs by the use of polarizing plates, semi- or non-polar crystal growth, and introducing nanostructures, have been reported.[2-5]

A dichromatic polarizing plate composed of an iodine-doped polymer has been widely used to control the polarization characteristics of LEDs. The polarization ratio, defined as the ratio of the

intensity of two orthogonal polarizations, has reached nearly 100 in the visible region. The filter is too large for integrated devices, exceeding one square centimeter in size, and most incident photons are absorbed in the polymer. Several groups have reported polarized emission from non- or semi-polar GaN-based LEDs, with polarization ratios as high as 8 in the wavelength region from 480 to 510 nm.[2-4] Emission power from non- or semi-polar GaN-based LEDs is lower than that from LEDs grown on c-plane (0001) sapphire, because of the comparatively poor quality of heteroepitaxial GaN films grown on the r-plane (1102). Lai *et al.* reported on polarized emission from conventional LEDs using photonic crystals.[5] While the polarization ratio at 470 nm reached as high as 5, the complex design of the device required many processes for fabrication.

Another technique attempted to achieve integrated polarization-controlling devices is the modification of conventional GaN-based LEDs with a dielectric sub-wavelength grating (SWG). In the SWG, an eigenmodes are defined as the solution of Maxwell's equations in the periodic refractive index distribution. Two kind of modes exist so called transverse electric (TE) and transverse magnetic (TM) mode, and the different interaction between modes in both groups results in different grating response for both polarizations. For carefully chosen grating parameter, destructive interference between the modes occur and results in high reflectivity, hence absorption of the material is one thing and the grating transmittance is the other. [6-15] In our previous study, we demonstrated highly polarized emission from a conventional GaN-based LED using an SWG in the 365-nm (UV) wavelength region.[13] The optical characteristics were analyzed and discussed using a typical rectangular grating shape.[6-15] The grating side slope, which requires very fine pitch, is sensitive to the fabrication conditions, including lithographic, crystal growth, evaporation, and etching conditions; the resultant grating shape is not always

rectangular.[16-18] The influence of this deviation from the rectangular shape on the SWG's polarization characteristics must be considered for effective design.

In this study, we investigated the emission from a GaN-based LED with a low-contrast dielectric SWG (SiO_2-SWG), because SiO_2-SWG has narrow-bandwidth polarization selectivity without photon absorption and is thus suitable for integrated polarization-controlling devices.[6] The low-contrast SWG means the refractive index of SiO_2 is not so higher than that of air. First, the electromagnetic field distribution within the SiO_2-SWG was theoretically calculated by the finite-difference time-domain (FDTD) method in order to estimate the influence of the grating shape on the polarization characteristics of the LED emission with the SiO_2-SWG. Next, a trapezoid-shaped SiO_2-SWG structure was fabricated on the surface of a GaN-based blue LED using electron-beam lithography. Electroluminescence (EL) spectra from the LED with the SiO_2-SWG were measured, and the polarization characteristics of the emission were discussed.

2   Theoretical investigation

The interaction between modes within the SWG dominates the polarization characteristics of the SWG. We predicted that the SWG polarization characteristics depend on deviation from the rectangular grating shape, because deviation creates different eigenstate modes.[6-9] To estimate the influence of shape deviation, we investigated electromagnetic field distribution using the FDTD method. The FDTD method is for solving Maxwell's equation using finite difference approximation. The flow chart of FDTD calculation is shown in Fig.1. The simulation region is divided into the rectangle cells and time is broken up into incremental time step Δt. First, the electric field component (E) at the specific time t is calculated in the divided rectangle cell. Second, the magnetic field component (H) at $t+\Delta t/2$ is calculated using the electric field component at t. Finally, the electric field component at $t+\Delta t$ is also calculated using the magnetic field component at $t+\Delta t/2$. Repeating this calculation cycle in each rectangle cells, we can obtain the electromagnetic response of the structure in the simulation region.

Figure 2 shows the cross-section of the numerical model used to investigate electromagnetic field distribution. In this model, the SiO_2-SWG is arranged on the p-type GaN of the LED surface. Grating pitch, height, and bottom side length, defined in the Fig. 2, are set to $\Lambda = 430$ nm, $h = 200$ nm, and $W_2 = 215$ nm, respectively. The width of the top side of grating stripe is assigned W_1. The symbol λ_0 represents the incident wavelength in air. The refractive indices of SiO_2 (n_{SiO2}) and p-type GaN (n_{GaN}) employed are taken from the literature.[19-21] For example, $n_{SiO2} = 1.484+0i$, $n_{GaN} = 2.366+0.0116i$ for 400 nm, $n_{SiO2} = 1.482+0i$, $n_{GaN} = 2.324+0.0059i$ for 420 nm, $n_{SiO2} = 1.481+0i$, $n_{GaN} = 2.313+0i$ for 440 nm, $n_{SiO2} = 1.479+0i$, $n_{GaN} = 2.313+0i$ for 460 nm,

n_{SiO2} = 1.479+0i, n_{GaN} = 2.313+0i for 480 nm were used. We assume that "exp (-iωt)" indicates the time dependence of the incident light propagating to plus z direction. The grating was simulated as having infinite length along the y direction. The periodic and perfectly matched layer boundary conditions were used in the x and z directions, respectively. The simulation region was divided into 2 nm × 2 nm cells to investigate the electromagnetic field. The incremental time step in this simulation Δt was 0.47 fs. The incident plane wave was either TE-polarized or TM-polarized. In case of TE-polarization, the electric field vector is parallel to the grating stripes and in case of TM-polarization, the electric field vector is perpendicular to the grating stripe. The incident wave propagated from the GaN side to the air side. The transmitted light intensity through the SiO_2-SWG was calculated in the observation plane, placed at the air side for the TE- and TM-polarization. The width of the top side of the grating stripe W_1 = 0 nm, 10 nm, 100 nm, and 215 nm were used in order to clarify the dependence of the SWG polarization ratio on the grating shape. The bottom width of the grating stripe W_2 is kept constant, while the top width is changed.

The dependence of the SWG polarization ratio on the grating shape is shown in Fig. 3 as a function of the incident wavelength and summarized in Table 1. The polarization ratio has a peak around 440 nm for each grating shape, while the intensity strongly depends on W_1. The peak in the case of W_1 = 100 nm exceeds those in other grating shapes, reaching to a polarization ratio approaching 5. As W_1 decreases from 100 nm to 0 nm, the peak value dramatically decreases. The peak for W_1 = 0 nm is lower than half the height of that for W_1 = 100 nm. The distribution of Poynting vector value (which is defined as z component of Re[$\boldsymbol{E} \times \boldsymbol{H^*}$]) at a certain time for TE incidence is shown in Fig. 4. The light in the case of the grating with W_1 = 215 nm is confined to the high-refractive-index region in the grating structure. The confinement of the light becomes

weaker with decreasing W_1, and the light eventually penetrates into the air gap region. The transmittance of TE polarized light also varies with variations of the grating shape. This can be explained by the shift of the low-transmittance resonance condition due to the different eigenstates. If the modes are anti-phase and cancel each other's amplitudes, a low-transmittance resonance condition is created. [9] In this case, the low-transmittance condition is formed with TE-polarized light. Deviation from rectangular grating shapes modifies the modes' eigenstates, and the result is the varying degree of confinement of the light, and the resonance conditions with W_1 = 0 nm, 10 nm, and 100 nm differ from that in the rectangular grating (where W_1 = 215 nm). As a result, the transmittance of TE-polarized light, for which the low-transmittance resonance condition is formed, varied with decreasing W_1.

3   Experimental procedure

The SiO_2-SWG was fabricated on a GaN-based LED. The LED structure, emitting in the 430 nm to 440 nm wavelength region, was grown on a c-plane sapphire substrate by a metalorganic chemical vapor deposition method. The structure comprises layers of *p*-type GaN, *p*-type AlGaN, InGaN/GaN multi-quantum well, *n*-type AlGaN, *n*-type GaN, and undoped GaN on the sapphire substrate.[22] The emission peak is around 430 to 440 nm. The SiO_2-SWG was fabricated using electron-beam lithography and evaporation. First, electron-beam resist (ZEP-520A) was diluted with methoxybenzene (anisole) to a 1:1 solution, and the resist film was spin-coated onto the LED surface at 2000 rpm for 90 s to a thickness of about 200 nm. The resist-coated LED was baked on a hotplate at 180 °C for 3 min. Secondly, the grating pattern, with a 430-nm pitch and 200-nm grating bar width, was drawn on the LED's top surface using an electron beam at 50 kV and 100 pA. The grating pattern was developed by n-amyl acetate (ZED-50N) at 20 °C for 15 s. After developing, a 200 nm SiO_2 film was evaporated onto the grating pattern using an electron beam at a chamber pressure of 2.7×10^{-3} Pa, and the resist film was removed by dimethyl sulfoxide. Finally, a 20-nm-thick Au/Ni *p*-contact film was evaporated as the electrode.

4   Result and discussions

A cross-sectional scanning electron microscope (SEM) view of the SiO_2-SWG on the surface of the GaN-based blue LED is shown in Fig. 5. The resultant grating pitch, bottom width, and height are 430 nm, 215 nm, and 200 nm, respectively. The top side width of the grating is about 10 nm, providing a trapezoidal resultant grating shape. The trapezoid shape is typical of the fabricated SiO_2 stripe.[18] The EL spectra at a forward current I_F of 10 mA from the blue LED with SiO_2-SWG are shown in Fig. 6. The open and filled circles indicate the intensities of TM- and TE-polarized emission, respectively. The TM- and TE-polarized spectra were measured by rotating the polarizer placed in front of the blue LED. The spectra show a polarized emission from the blue LED with SiO_2-SWG in the wavelength region from 420 nm to 450 nm. The peak polarization ratio reaches about 3.2 at the wavelength of 440 nm. The experimental polarization ratio exceeds that numerically predicted by FDTD method.

In the resultant SWG, the refractive index of the grating depends on the fabrication process. The dependence of the SWG polarization characteristics on the actual refractive index of grating should be considered for accurate analysis of the experimental results. The actual n_{SiO2} of the SiO_2 evaporated by the e-beam depends on the evaporation conditions, and n_{SiO2} ranges from 1.46 to 1.56 at the 440 nm wavelength.[23] We deduce that the higher polarization ratio than that numerically predicted might be caused by the change of n_{SiO2}. To verify this consideration, we investigated the dependence of the polarization characteristics of the LED's emission on n_{SiO2} using the FDTD method with the model shown in Fig. 2. For the calculation, we set W_I equal to 10 nm. The calculated polarization characteristics of the emission are shown in Fig. 7 as a function of n_{SiO2}. The open and filled circles show the transmittance through the SiO_2-SWG for

the case of perfectly TM- or TE-polarized incident light. Crosses indicate the polarization ratio at different refractive indices. The transmittance of TM-polarized light is almost insensitive to variations in n_{SiO2}. However, the transmittance of TE-polarized light linearly decreases with increasing n_{SiO2}. The polarization ratio also linearly increases from 2.4 to 3.4 with increasing n_{SiO2}. When n_{SiO2} is set to 1.55, the calculated polarization ratio agrees with the experimental value. The agreement between the calculated polarization characteristics with actual n_{SiO2} and the experimental characteristics can be explained as follows. The light velocity in the high-refractive-index region is slower than that in the low-refractive-index material. Thus, the electromagnetic field distribution, eigenstates, and low-transmittance resonance conditions all vary with increasing n_{SiO2}. The results indicate that SWG design considering the variety of eigenstates may serve to develop high-performance polarization-controlling devices.

5 Conclusions

In conclusion, we investigated the dependence of the shape of the SWG on the different eigenstate modes within an SWG. The electromagnetic field distribution within the SiO_2-SWG calculated by FDTD methods indicated that deviation from standard rectangular SWG shapes creates different eigenstates, and the low-transmittance resonance condition of the SWG strongly depends on the grating shape. We fabricated a trapezoidal SiO_2-SWG on a GaN-based blue LED and obtained polarized emission from the LED. The polarization ratio reached 3.2 at an incident wavelength of 440 nm. The experimental polarization characteristics of the emission agreed with those theoretically predicted by considering the resultant n_{SiO_2} as affected by fabrication conditions, and we demonstrated that the shape of the SWG strongly modifies the polarization characteristics of LED emissions with a SiO_2-SWG structure.

References

1. S. Fujita, "Wide-bandgap semiconductor materials: For their full bloom,"*Jpn. J. Appl. Phys.* **54**(3), 030101 (2015).

2. S. You, T. Detchprohm, M. Zhu, W. Hou, E. A. Preble, D. Hanser, T. Paskova, and C. Wetzel, "Highly Polarized Green Light Emitting Diode in m-Axis GaInN/GaN," *Appl. Phys. Express* **3**(10), 102103 (2010).

3. N. F. Gardner, J. C. Kim, J. J. Wierer, Y. C. Shen, and M. R. Krames, "Polarization anisotropy in the electroluminescence of m-plane InGaN-GaN multiple-quantum-well light-emitting diodes," *Appl. Phys. Lett.* **86**, 111101 (2005).

4. T. Koyama, T. Onuma, H. Masui, A. Chakraborty, B. A. Haskell, S. Keller, U. K. Mishra, J. S. Speck, S. Nakamura, S. P. DenBaars, T. Sota, and S. F. Chichibu, "Prospective emission efficiency and in-plane light polarization of nonpolar *m*-plane $In_xGa_{1-x}N$/GaN blue light emitting diodes fabricated on freestanding GaN substrates," *Appl. Phys. Lett.* **89**, 091906 (2006).

5. C. F. Lai, J. Y. Chi, H. H. Yen, H. C. Kuo, C. H. Chao, H. T. Hsueh, J. F. Trevor Wang, C. Y. Huang, and W. Y. Yeh, "Polarized light emission from photonic crystal light-emitting diodes," *Appl. Phys. Lett.* **92**, 243118 (2006).

6. C. J. Chang-Hasnain, "High-contrast grating as a new platform for integrated optoelectronics," *Semicond. Sci. Technol.* **26**(1), 014043 (2011).

7. Y. Zhou, M. C. Y. Huang, C. Chase, V. Karagodsky, M. Moewe, B. Pesala, F. G. Sedgwick, and C. J. Chang-Hasnain, "High-Index-Contrast Grating (HCG) and Its Applications in Optoelectronic Devices," *IEEE J. Sel. Top. Quantum Electron.* **15**(5), 1485-1499 (2009).

8. V. Karagodsky, B. Pesala, F. G. Sedgwick, and C. J. Chang-Hasnain, "Dispersion properties of high-contrast grating hollow-core waveguides," *Opt. Lett.* **35**(24), 4099-4101 (2010).

9. V. Karagodsky, F. G. Sedgwick, and C. J. Chang-Hasnain, "Theoretical analysis of subwavelength high contrast grating reflectors," *Opt. Express* **18**(16), 16973-16988 (2010).

10. Y. Laaroussi, C. Chevallier, F. Genty, N. Fressengeas, L. Cerutti, T. Taliercio, O. Gauthier-Lafaye, P. F. Calmon, B. Reig, J. Jacquet, and G. Almuneau, "Oxide confinement and high contrast grating mirrors for Mid-infrared VCSELs," *Opt. Mater. Express* **3**(10), 1576-1585 (2013).

11. T. T. Wu, Y. C. Syu, S. H. Wu, W. T. Chen, T. C. Lu, S. C. Wang, H. P. Chiang, and D. P. Tsai, "Sub-wavelength GaN-based membrane high contrast grating reflectors," *Opt. Express* **20**(18), 20551-20557 (2012).

12. C. Chase, Y. Rao, W. Hofmann, and C. J. Chang-Hasnain, "1550nm high contrast grating VCSEL," *Opt. Express* **18**(15), 15461-15466 (2010).

13. Y. Takashima, R. Shimizu, M. Haraguchi, and Y. Naoi, "Polarized emission characteristics of UV-LED with subwavelength grating," *Jpn. J. Appl. Phys.* **53**(7), 072101 (2014).

14. H. Li, W. Li, A. Wu, C. Qiu, Z. Sheng, X. Wang, S. Zou, and F. Gan, "Broadband compact reflector based on all-dielectric subwavelength nanoparticle chains: reflecting lights beyond normal incidence with a very high reflectivity," *Opt. Eng.* **52**(6), 068001 (2013).

15. M. Gebski, M. Dems, J. Chen, Q. J. Wang, D. H. Zhang, and T. Czyszanowski, "The Influence of Imperfections and Absorption on the Performance of a GaAs/AlOx High-Contrast Grating for Monolithic Integration With 980nm GaAs-Based VCSELs," *J. Lightwave Technol.* **31**(23) 3853-3858 (2013).

16. Y. Kawaguchi, S. Nambu, H. Sone, T. Shibata, H. Matsushima, M. Yamaguchi, H. Miyake, K. Hiramatsu, and N. Sawaki, "Selective Area Growth of GaN Using Tungsten Mask by Metalorganic Vapor Phase Epitaxy," *Jpn. J. Appl. Phys.* **37**(7B), L845-L848 (1998).

17. S. Zhou, B. Cao, S. Liu, "Optimized ICP etching process for fabrication of oblique GaN sidewall and its application in LED," *Appl. Phys. A* **105**(2), 369-377 (2011).

18. S. Heikman, S. keller, S. P. Denbaars, U. K. Mishra, F. Bertram, and J. Christen, "Non-planar Selective Area Growth and Characterization of GaN and AlGaN," *Jpn. J. Appl. Phys.* **42**(10), 6276-6283 (2003).

19. D. Brunner, H. Angerer, E. Bustarret, F. Freudenberg, R. Hopler, R. Dimitrov, O. Ambacher, and M. Stutzmann, "Optical constants of epitaxial AlGaN films and their temperature dependance," *J. Appl. Phys.* **82**(10), 5090-5096 (1997).

20. T. Iwanaga, T. Suzuki, S. Yagi, and T. Motooka, "Optical absorption properties of Mg-doped GaN nanocolumns," *J. Appl. Phys.* **98**(10), 104303 (2005).

21. L. Gao, F. Lemarchand, and M. Lequime, "Exploitation of multiple incidences spectrometric measurements for thin film reverse engineering," *Opt. Express* **20**(14), 15734-15751 (2012).

22. Y. Naoi, M. Matsumoto, T. Tan, M. Tohno, S. Sakai, A. Fukano, S. Tanaka, "GaN-based light emitting diodes with periodic nano-structures on the surface fabricated by nanoimprint lithography technique" *Phys. Status Solidi C* **7**(7-8), 2154-2156 (2010).

23. M. Jerman, Z. Qiao, and D. Mergel, "Refractive index of thin films of SiO_2, ZrO_2, and HfO_2 as a function of the films' mass density," *Appl. Opt.* **44**(15), 3006-3012 (2005).

Biographies

Biographies are not available.

Tables

Table 1 Summarized polarization ratio of the SiO_2-SWG at $\lambda_0 = 440$ nm.

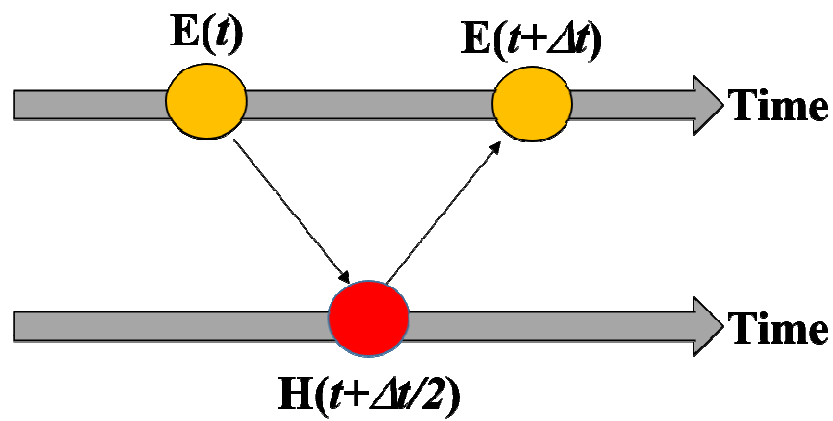| W_1 [nm]	Polarization ratio
0	1.93
10	2.16
100	4.95
215	4.18

Caption List

Fig. 1 Flow chart of FDTD method. The electric field component in the divided rectangle cells at specific time t is calculated. Based on the electric filed at t, the magnetic field component at t+Δt/2 is calculated. The electric field at t+Δt is calculated using the magnetic field at t+Δt/2. Repeating this calculation cycle in each rectangle cells, the electromagnetic response of the structure in the simulation region can be obtained.

Fig. 2 Numerical model for investigating of electromagnetic field distribution. The SiO₂-SWG is placed on the GaN. The symbol Λ, h, W_1, W_2, indicates the grating pitch, the grating height, the width of the top side of the grating stripe, and the bottom width of the grating strip, respectively. The symbol λ_0 indicates incident wavelength, and the incident wave propagates from input side (GaN) into output side (air). The grating strip is infinity for y direction. The PML boundary condition is used z direction, and the periodic boundary condition is used for the x direction. The simulation region is divided into 2 nm × 2 nm rectangle. The incremental time step is 0.47 fs.
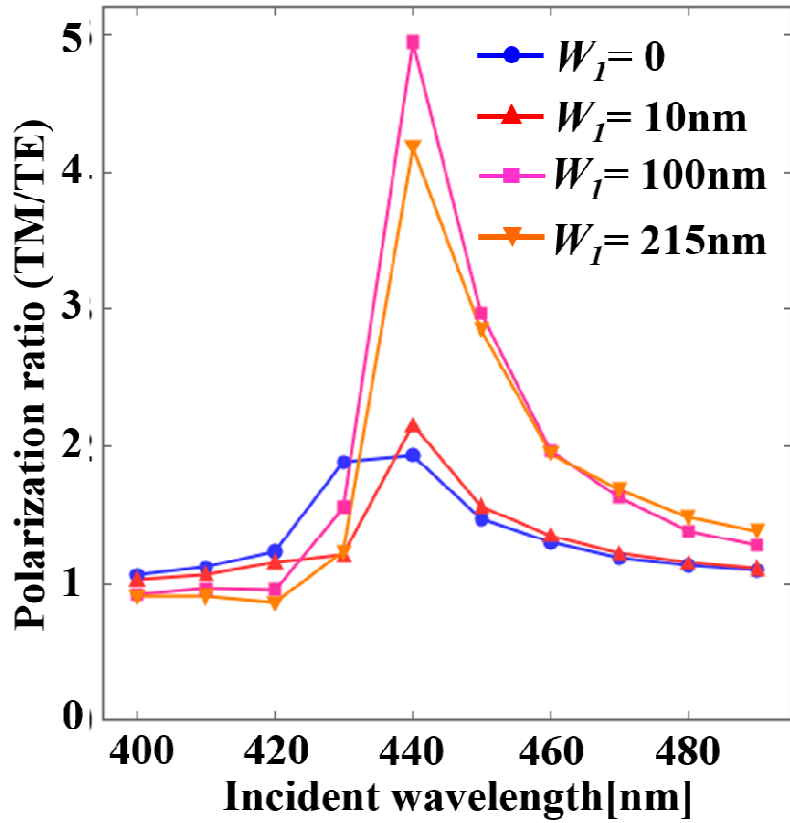
Fig. 3 The SiO$_2$-SWG polarization ratio as a function of the incident light wavelength with $W_1 =$ 0 nm, 10 nm, 100 nm, and 215 nm ($\Lambda = 430$ nm, $h = 200$ nm, $W_2 = 215$ nm). The polarization ratio has a peak around 440 nm for all grating shapes. The peak intensity strongly depends on W_1. The peak in the case of $W_1 = 100$ nm exceeds those in other grating shapes, and the value reached to a polarization ratio approaching 5. The peak value dramatically decreases with the decreasing W_1, and the peak for $W_1 = 0$ nm is lower than half of that for $W_1 = 100$ nm.
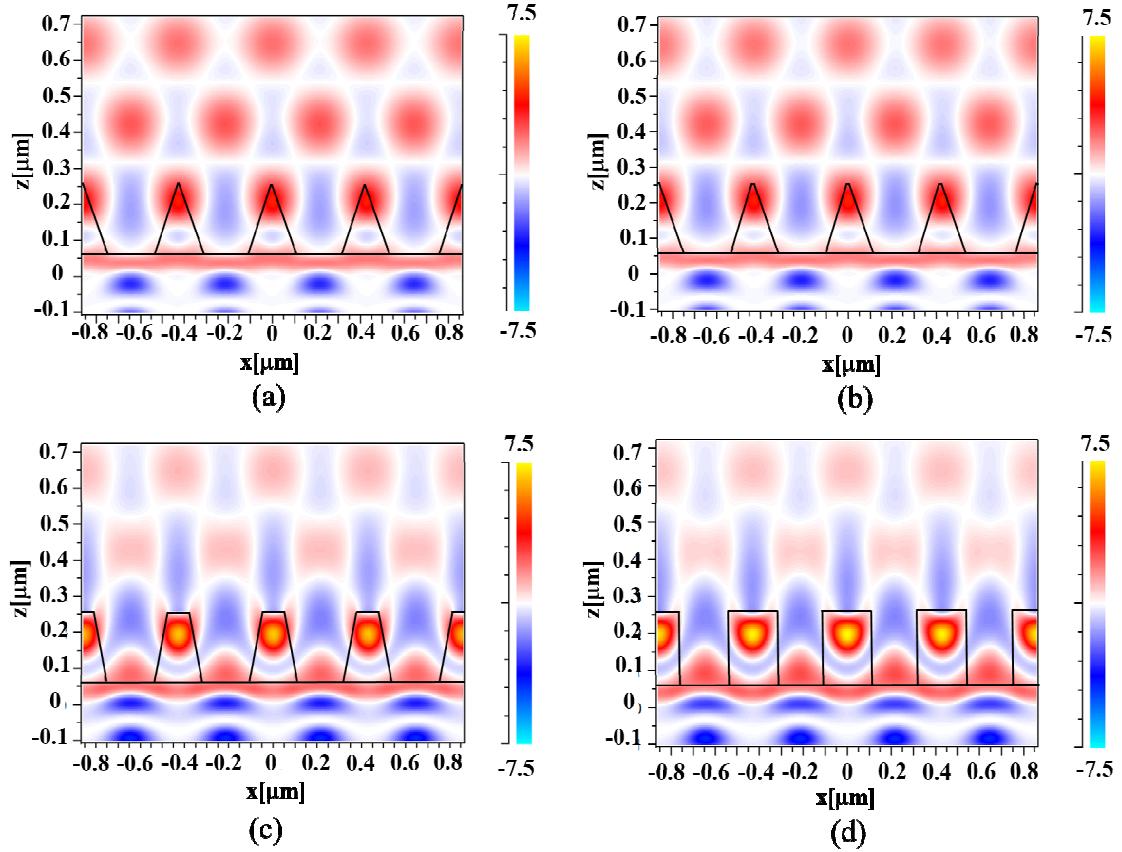
17

Fig. 4 The distribution of Poynting vector value at a certain time for TE incidence ($\lambda_0 = 440$ nm, $\Lambda = 430$ nm, $h = 200$ nm, $W_2 = 215$ nm). (a)$W_1 = 0$ nm. (b) $W_1 = 10$ nm. (c) $W_1 = 100$ nm. (d) $W_1 = 215$ nm. For the case of the grating with $W_1 = 215$ nm, the light is strongly confined to high-refractive-index region (SiO_2) in the grating structure. The confinement of light becomes weaker with decreasing W_1, and the transmittance also varies with variations of the grating shape.
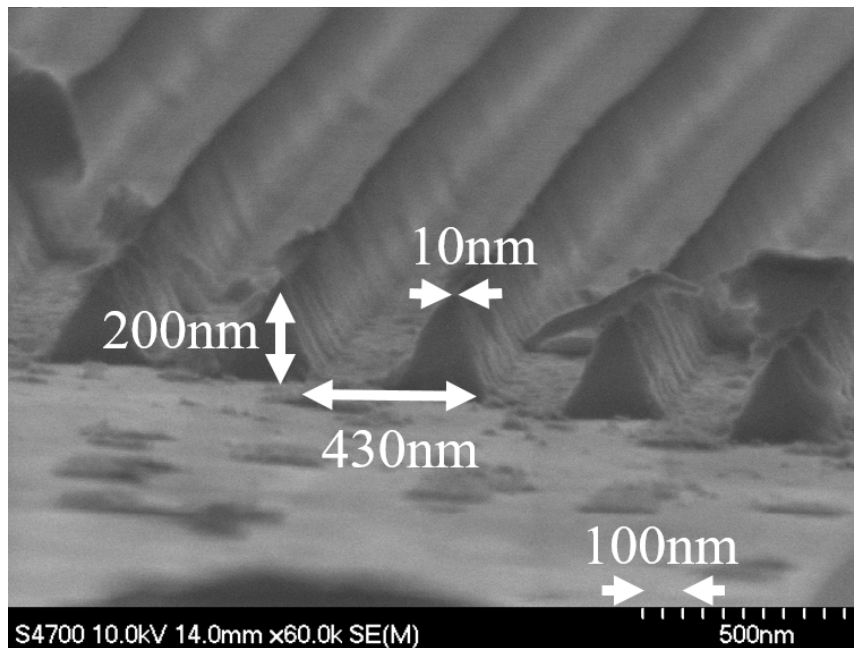
Fig. 5 Cross-sectional scanning electron microscope view of the SiO$_2$-SWG fabricated on a GaN-based blue light-emitting diode (LED). The grating pitch Λ, grating height h, the width of the bottom side of grating strip W_2, and the width of the top side of the grating strip W_1 are 430 nm, 200 nm, 215 nm, and 10 nm, respectively.
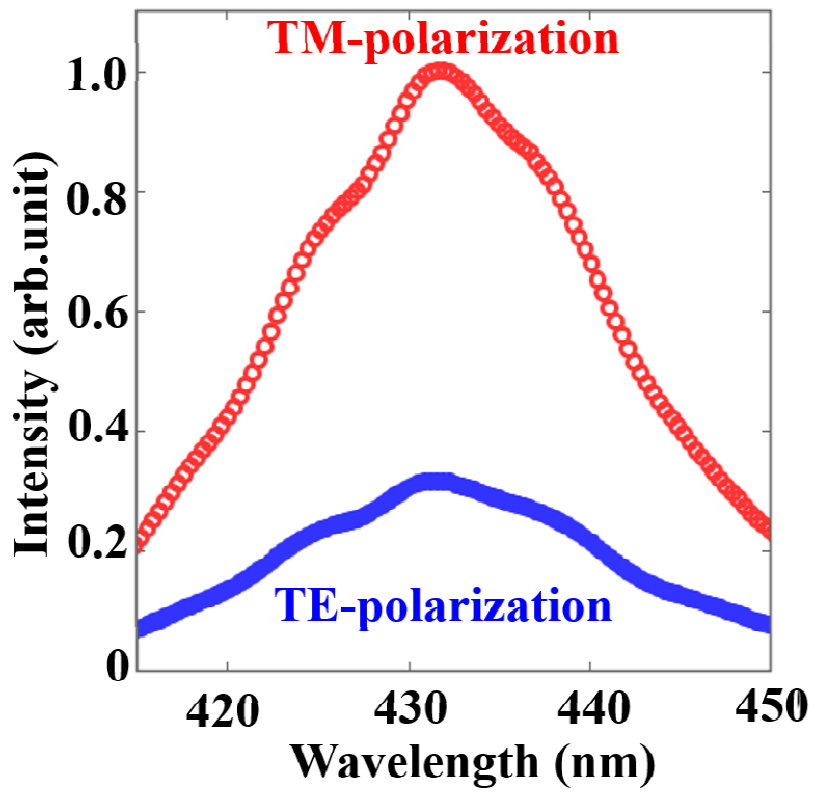
Fig. 6 Emission spectra from the GaN-based blue LED with SiO_2-SWG for I_F = 10 mA. The polarized emission from the blue LED with SiO-SWG in the wavelength region from 420 nm to 450 nm. The peak polarization ratio is 3.2 at the wavelength of 440 nm.
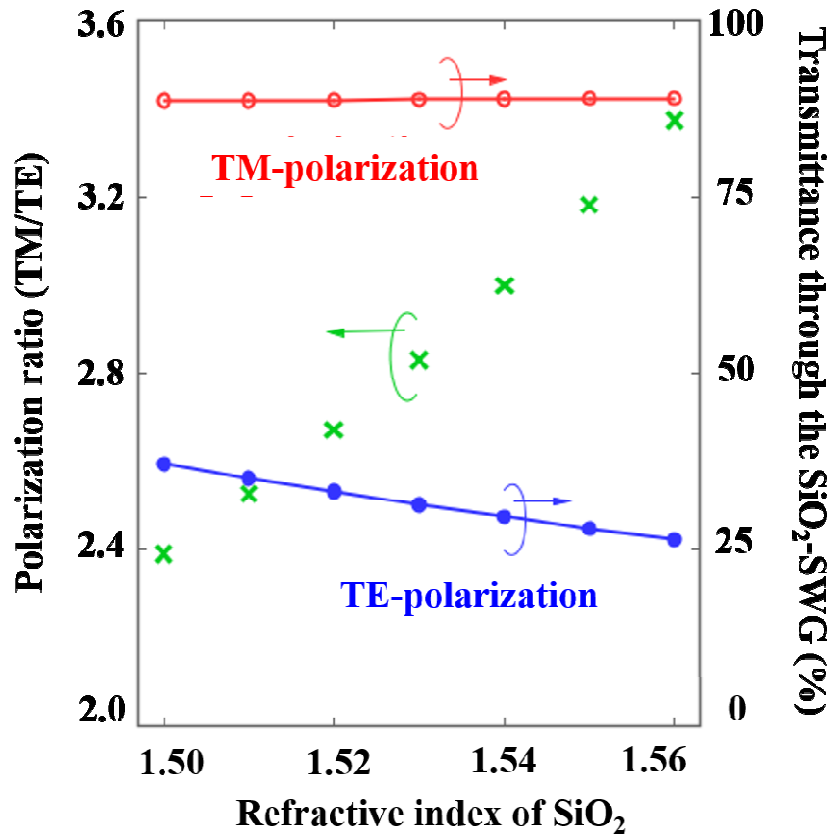
Fig. 7 Dependence of LED emission's polarization characteristics on n_{SiO2} at $\lambda_0 = 440$ nm. The transmittance of TM-polarized light is almost insensitive to variations in n_{SiO2}. The transmittance of TE-polarized light decreases with increasing n_{SiO2}. The polarization ratio also linearly increases from 2.4 to 3.4 with increasing n_{SiO2}. The calculated polarization ratio at $n_{SiO2} = 1.55$ agrees with the experimental value.